Title	Petrography, K-Ar age, and chemistry of Yoshino-dai lavas in the Aira caldera
Author(s)	INOUE, Hisashi; ITAYA, Tetsumaru; TATSUMI, Yoshiyuki
Citation	Bulletin of the Disaster Prevention Research Institute (1994), 44(4): 175-190
Issue Date	1994-12
URL	http://hdl.handle.net/2433/125006
Right	
Type	Departmental Bulletin Paper
Textversion	publisher

Bull. Disas. Prev. Res. Inst., Kyoto Univ., Vol. 44, Part 4, No. 384, December, 1994

Petrography, K-Ar age, and chemistry of Yoshino-dai lavas in the Aira caldera

By Hisashi INOUE, Tetsumaru ITAYA, and Yoshiyuki TATSUMI

(Manuscript received on Sep. 6, 1994, revised on Oct. 22, 1994)

Abstract

The Aira caldera was formed about 22,000 years ago in association with large-scale pyroclastic eruptions of more than 400 km^3 felsic ejecta. Petrography was described and major/trace element compositions and K-Ar ages were determined for Aira precaldera lavas in the Yoshino-dai area, in order to examine mechanisms by which a series of the Aira precaldera and climactic magmas were produced. Precaldera lavas in the Yoshino-dai area mainly consist of augite-olivine basalt and two-pyroxene andesite, as previous workers indicated. K-Ar ages of precaldera basalts and andesites are >0.5 Ma and, in contrast, K-Ar age of precaldera rhyolite is <0.5 Ma and eruptions of precaldera dacites and minor pyroclastic flows may have occurred after $\sim$ 0.5 Ma. The precaldera and climactic ejecta show a single chemical trend with the cusp at $SiO^2 \sim 65$ wt. % for some elements. It follows that a series of Aira precaldera magmas was not produced by a single process such as fractional crystallization from basaltic magmas or two-end-member mixing between basaltic magmas and rhyolitic magmas. The generation of a series of Aira precaldera magmas requires at least two processes; production of basaltic to andesitic magmas before $\sim$ 0.5 Ma and of dacitic to rhyolitic magmas after $\sim$ 0.5 Ma. The possibility that the state of the magmatic system beneath the Aira caldera may have changed at $\sim$ 0.5 Ma remains.

1. Introduction

Large volumes of felsic rocks, which are generally related to caldera formation, are one of the most important constituents both in island arc and continental margin settings. Elucidation of the genesis of such magmas may therefore provide a key to understanding magma generation in subduction zones and subsequent formation of the continental crust.

In order to clarify the origin of caldera-related felsic magmas, it should be important to discuss the genetic relation between climactic ejecta and precaldera ejecta. This is especially true for precaldera basalt because precaldera basaltic magmas, which are possibly mantle-derived, may supply both heat and mass to intra-crustal magmatic systems (Hildreth, 1981).

The Aira caldera was formed about 22, 000 years ago in association with eruptions amounting to more than 400 km^3 felsic ejecta (Aramaki, 1984). In the Aira caldera, precaldera lavas including those of basaltic compositions are distributed in Yoshino-dai

and Ushine areas (Figs. 1, 2). Geological and petrographical investigations of these precaldera lavas were conducted by Oki and Hayasaka (1970), Yamaguchi (1975), and Kobayashi et al. (1977). However, no study on the generation of the felsic magma in connection with the precaldera ejecta has yet been carried out.

This paper presents the petrography, K-Ar ages, and major/trace element compositions for the Aira precaldera lavas in the Yoshino-dai area and then discusses mechanisms for production of a series of the Aira precaldera and climactic magmas.

2. Geology and Petrography

Geological and petrographic descriptions of the Yoshino-dai area were given by Oki and Hayasaka (1970), Yamaguchi (1975), and Inoue (1992). Oki and Hayasaka (1970) showed that stratigraphic units in the southern part of the Yoshino-dai area can be divided into four major geographical units as follows (in ascending order):

1) The volcanic rock bodies probably of the latest Neogene age—Ryugamizu Andesite and Mifune Rhyolite.
2) Late Pliocene or Early Pleistocene volcanic and sedimentary rocks showing intimate relation with each other—Hiramatsu Andesite (renamed in this paper), Mifune Formation, Shirahama Basalt, Muregaoka Andesite, and Kekura Formation.
3) Several pyroclastic flow deposits and the interbedded fossil-bearing strata distributed almost all over the area—Yoshino pumice flow, Kogashira Formation, Shimokado pumice flow, Oyamada Formation, Inuzako pumice flow, Shiroyama Formation, Tatsuo Formation, Kamo pumice flow, Nagaida pumice flow, and Sakamoto pumice flow (corresponding to Ito pyroclastic flow deposit)
4) Holocene pumice bed and volcanic ash.

The first author carried out field surveys around the northern parts of the Yoshino-dai area. Only sampling was done for the southern parts. Here, the geology and petrography only of lavas for which chemical compositions could be obtained have been modified and described again. A geological map of the Yoshino-dai area is shown in Fig. 3. Modal compositions by 2,000-point counting are shown in Table 1.

Mifune rhyolite (Hypersthene-hornblende rhyolite)

This lava flow is distributed for ~ 1 km north of the Mifune shrine. The lithofacies of the flow vary significantly northwards from spherulitic rocks, gray banded tuff, obsidian, glassy tuff, to rhyolite.

The flow as well as Ryugamizu andesite lies on the lowest positions in the Yoshino-dai area, though the stratigraphic relation between these flows is not clear. The Mifune rhyolite lava flow is covered with the Mifune formation and Hiramatsu andesite, all of which are overlain by the Kekura formation, as Oki and Hayasaka (1970) reported.

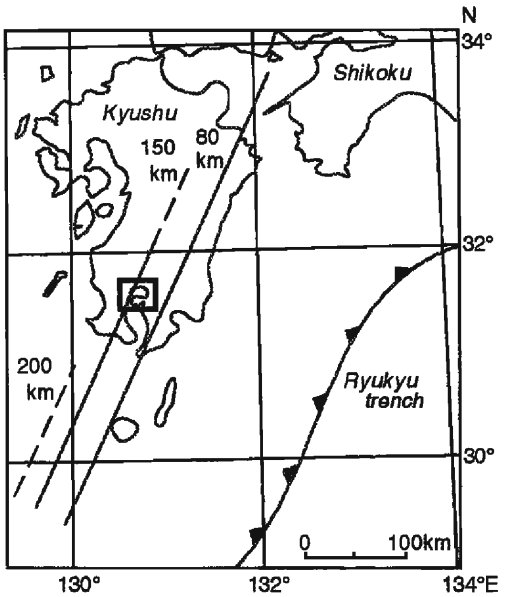

Fig. 1. Tectonic setting of southern Kyushu. Isobaths of intermediate-depth earthquakes after Nagamune (1987). *Square* corresponds to the area of Fig. 2.

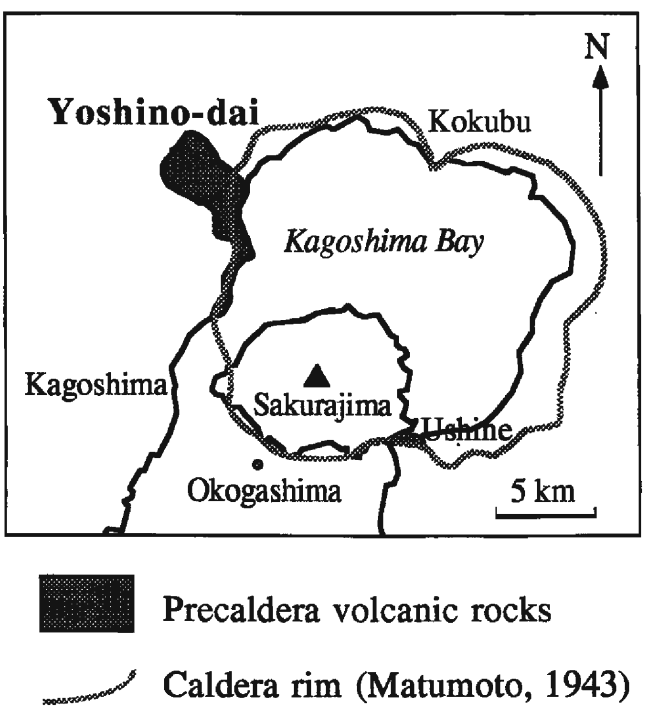

Fig. 2. Index map showing the caldera rim and the distribution of the precaldera volcanic rocks.

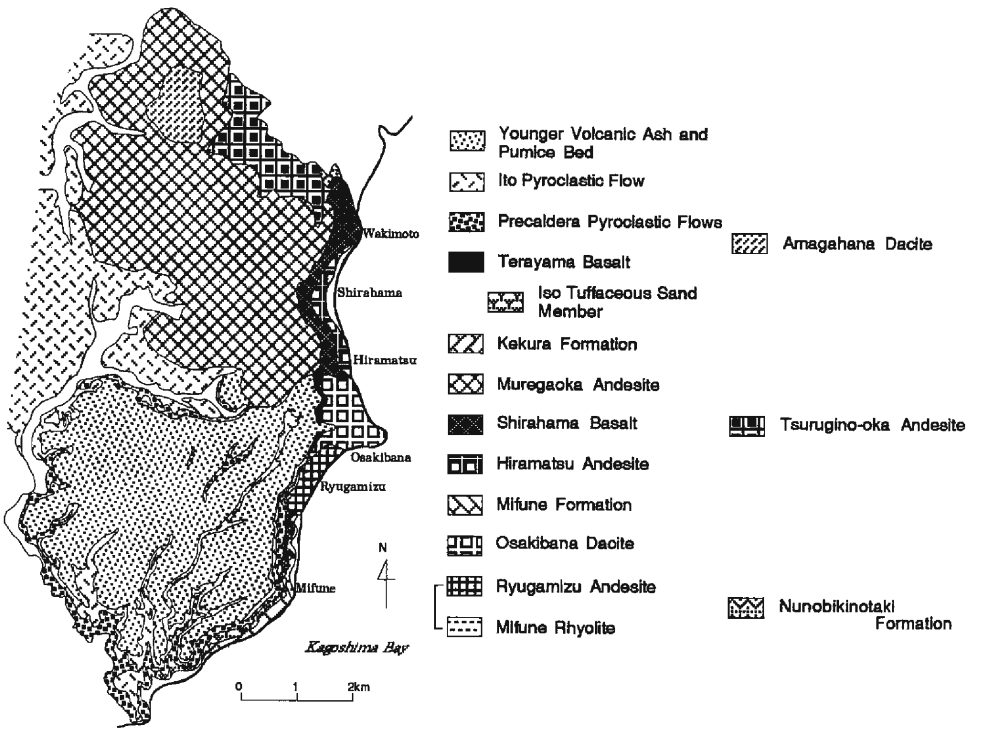

Fig. 3. Geological map of Yoshino-dai area. Geology in the southern part after Oki and Hayasaka (1970) and in the northern part after Inoue (1992), partly modified.

Table 1. Modal compositions by 2,000 point counting and minerals in groundmass for the precaldera lavas in the Yoshino-dai area.

Lava name	Sample	pl	aug	hy	ol	hb	Ti-mg	GM	minerals of GM
Amagahana dacite	AG-85	18.6	-	1.2	-	4.5	0.7	75.0	glassy
Terayazma basalt	AR-4.1	38.7	tr.	-	1.4	-	-	60.0	pl, px, Ti-mg
Muregaoka andesite	MY-09	31.6	2.4	3.1	1.0	-	1.5	60.3	pl, aug, Ti-mg, glass
Tsurugino-oka andesite	SG-92	26.8	4.2	3.0	-	tr.	1.9	64.1	pl, Ti-mg, glass
Shirahama basalt	AR-1	37.6	0.2	-	1.8	-	-	60.6	pl, cpx, Ti-mg
Hiramatsu andesite	SH-43	17.1	0.5	0.8	-	-	0.4	81.4	pl, Ti-mg, glass
Osakibana basaltic dike	AR-3.2	30.2	0.7	-	4.9	-	-	64.3	pl, cpx, Ti-mg
Osakibana dacite	AR-3.3	9.7	0.7	0.6	-	-	0.5	88.5	cryptocrystalline
Ryugamizu andesite	AR-33	31.6	5.8	2.5	-	-	1.5	58.7	cryptocrystalline

Xenoliths were not counted.

Abbreviations. pl:plagioclase, aug:augite, hy:hypersthen, ol:olivine, hb:hornblende, Ti-mg:titanomagnetite, GM:groundmass, px:pyroxene, cpx:clinopyroxene

Ryugamizu andesite (Hypersthene-augite andesite)

This lava flow is distributed from Osakibana to Ryugamizu. The flow is overlain by Shirahama basalt and Osakibana dacite, as Oki and Hayasaka (1970) reported.

Microscopically, the lava is porphyritic, in which the phenocryst phases are plagioclase, augite, hypersthene, and titanomagnetite. Plagioclase phenocrysts are euhedral or subhedral and <3.5 mm in length. They show zoning and twinning, and contain glass, titanomagnetite, augite, and hypersthene. Some contain a lot of glass. Augite phenocrysts are euhedral or subhedral, and usually <0.5 mm, but with a maximum of 3 mm in length. They show twinning and contain titanomagnetite and plagioclase. Hypersthene phenocrysts are euhedral or subhedral, <1.8 mm in length, and contain titanomagnetite and plagioclase. Titanomagnetite phenocrysts have irregular shapes and are <0.5 mm in length. Some phenocrysts form crystal clusters (glomeroporphyritic assemblage), composed of plagioclase (pl) + hypersthene (hy) + augite (aug) + titanomagnetite (Ti-mg) ± glass, pl, pl + hy + Ti-mg, and pl + aug + Ti-mg. Some large clusters 0.3-6 mm in length composed of pl + hy + aug + Ti-mg + glass also are found, in which the ratio of colored minerals is higher than the host rock. The groundmass is cryptocrystalline, in which plagioclase and titanomagnetite can be identified.

Hiramatsu andesite (Augite-hypersthene andesite)

This lava flow corresponds to 'Hiramatsu basalt' of Oki and Hayasaka (1970). Chemical composition of the lava ($SiO_2 \sim 60$ wt. %, see Table 3) shows that it must be renamed 'Hiramatsu andesite'.

The lava flow is distributed from Wakimoto to Hiramatsu and around Mifune. The Hiramatsu andesite lava flow may overlie Mifune rhyolite and the Mifune formation, and be overlain by Shirahama basalt and the Kekura formation, as Oki and Hayasaka (1970) reported.

Microscopically, the lava is porphyritic, in which the phenocryst phases are plagioclase, hypersthene, augite, and titanomagnetite. Both clear and honeycomb plagioclase phenocrysts are found. Both are euhedral or subhedral. Clear plagioclases are <1.5 mm and honeycomb plagioclases are <2 mm in length. The plagioclase phenocrysts show zoning and twinning, and contain glass, augite, and titanomagnetite. Hypersthene phenocrysts are subhedral, <1 mm in length, and contain plagioclase and titanomagnetite. Augite phenocrysts are subhedral and <1.2 mm in length, show twinning, and contain plagioclase and titanomagnetite. Titanomagnetite phenocrysts have irregular shapes and are <0.5 mm in length. Some phenocrysts form crystal clusters, composed of pl, aug + hy + Ti-mg + glass, and aug + pl + Ti-mg. The groundmass is intersertal with flow structure and composed of plagioclase, titanomagnetite, fine minerals, and glass.

Osakibana dacite (Hypersthene-augite dacite)

This lava flow corresponds to 'Osakibana andesite' of Oki and Hayasaka (1970).

Chemical composition of the lava ($SiO_2 \sim 66$ wt.%, see Table 3) shows that it must be renamed 'Osakibana dacite'.

The lava flow forms Osakibana and is intruded by basaltic dikes. The flow overlies Ryugamizu andesite and is overlain by the Kekura formation and Terayama basalt, as Oki and Hayasaka (1970) reported.

Microscopically, the lava is porphyritic, in which the phenocryst phases are plagioclase, augite, hypersthene, and titanomagnetite. Plagioclase phenocrysts are euhedral or subhedral and <1.3 mm in length, except for one 2.5 mm in length, the rim of which is dusty along the surface. They contain titanomagnetite. Augite phenocrysts are subhedral, <0.5 mm in length and contain titanomagnetite. Hypersthene phenocrysts are euhedral or subhedral, <1.5 mm in length, and contain titanomagnetite. Titanomagnetite phenocrysts have irregular shapes and are <0.5 mm in length. Some phenocrysts form crystal clusters, composed of pl + aug + Ti-mg, pl + aug + hy + Ti-mg, pl, pl + Ti-mg, and pl + hy + Ti-mg. The groundmass is cryptocrystalline, in which plagioclase and titanomagnetite can be identified. Xenoliths, 4 mm and 3 mm in length, which are composed of some 0.2-0.5 mm plagioclase and fine plagioclase, augite, titanomagnetite, and hypersthene, are found.

Osakibana basaltic dike (Augite-olivine basalt)

Some dikes with chilled margin intrude Osakibana dacite.

Microscopically, the dikes are porphyritic, in which the phenocryst phases are plagioclase, olivine, and augite. Plagioclase phenocrysts are euhedral or subhedral and <4 mm in length, show twinning, and contain fine minerals, chlorite, and calcite. Olivine phenocrysts are subhedral and usually 0.1-0.3 mm, at the maximum 1.3 mm in length. Most are altered into chlorite and iddingsite, some of which contain calcite. Augite phenocrysts are subhedral, <0.5 mm in length, and show twinning. The groundmass is intergranular and composed of plagioclase, augite, and titanomagnetite.

Shirahama basalt (Augite-olivine basalt)

This lava flow is distributed from Wakimoto through Shirahama to Hiramatsu and from Ryugamizu to Mifune. The flow probably overlies Hiramatsu andesite and may be overlain by Muregaoka andesite. The stratigraphic relation between Shirahama basalt and Tsurugino-oka andesite is not clear. In the south, Shirahama basalt overlies Ryugamizu andesite, as Oki and Hayasaka (1970) reported.

Microscopically, the lava is porphyritic, in which the phenocryst phases are plagioclase, olivine, and augite. Plagioclase phenocrysts are euhedral or subhedral and <3.5 mm in length, show twinning, and contain glass, titanomagnetite, and augite. Glass is devitrified into fine minerals. Some plagioclase phenocrysts form crystal clusters. Olivine phenocrysts are euhedral or subhedral and <1 mm in length. Most are altered into chlorite. Augite phenocrysts are subhedral, <0.5 mm in length, and show twinning. The groundmass is intergranular and composed of plagioclase, augite, and titanomagnetite.

Tsurugino-oka andesite (Hornblende-bearing hypersthene-augite andesite)

This lava flow is distributed in the northeast end of the Yoshino-dai area. The flow may be overlain by Muregaoka andesite.

Microscopically, the lava is porphyritic, in which the phenocryst phases are plagioclase, augite, hypersthene, titanomagnetite, and hornblende. Hornblende is rare. Both clear and honeycomb plagioclase phenocrysts are found. Both are euhedral or subhedral. Clear plagioclases are <3 mm and honeycomb plagioclases are <2 mm in length. The plagioclase phenocrysts show twinning and zoning and contain glass, augite, titanomagnetite, and hypersthene. Augite phenocrysts are subhedral and <0.5 mm in length, show twinning, and contain plagioclase and titanomagnetite. Hypersthene phenocrysts are subhedral, <2.5 mm in length, and contain titanomagnetite, plagioclase, and glass. Titanomagnetite phenocrysts have irregular shapes and are <0.7 mm in length. Hornblende phenocrysts are subhedral and ~ 0.3 mm in length, the rim of which is altered into opacite. Some phenocrysts form crystal clusters, composed of pl + aug + hy + Ti-mg + glass and pl. The groundmass is intersertal and composed of plagioclase, fine minerals, titanomagnetite, and glass. A xenolith ($\sim$ 1 cm) is found. It contains subhedral or anhedral phenocrysts of <0.4 mm augite, <1 mm plagioclase, and <0.5 mm hypersthene, which phenocrysts are set in the groundmass composed of plagioclase, titanomagnetite, and glass. Most phenocrysts in the xenolith are augite.

Muregaoka andesite (Olivine-bearing augite-hypersthene andesite)

This lava flow is distributed widely in the north of the Yoshino-dai area, having occasionally tuffacious xenoliths (2-3 cm). The flow may overlie Shirahama basalt and Tsurugino-oka andesite. In the south, Muregaoka andesite is overlain by Terayama basalt, as Oki and Hayasaka (1970) reported.

Microscopically, the lava is porphyritic, in which the phenocryst phases are plagioclase, hypersthene, augite, titanomagnetite, and olivine. Olivine is not found in all samples. Clear, dusty, and honeycomb plagioclase phenocrysts are found. Clear plagioclases are euhedral or subhedral and <4.5 mm in length. Dusty plagioclases are euhedral or subhedral and <5 mm in length. Honeycomb plagioclases are rare, subhedral, and <2.5 mm in length. The plagioclase phenocrysts show twinning and zoning and contain augite, hypersthene, titanomagnetite, and glass. Hypersthene phenocrysts are euhedral or subhedral, <2.5 mm in length, and contain plagioclase and titanomagnetite. Augite phenocrysts are euhedral or subhedral, show twinning, and contain plagioclase and titanomagnetite. Some parallel growths of augite and hypersthene are found. Titanomagnetite phenocrysts have irregular shapes and are <0.7 mm in length. Olivine phenocrysts are subhedral and usually <1 mm, at the maximum 0.4 mm in length. Most have reaction rims of pyroxene. Some are surrounded by fine plagioclase, augite, and titanomagnetite. Some phenocrysts form crystal clusters, composed of pl and pl + hy$\pm$aug + Ti-mg. The groundmass is intersertal and composed of plagioclase, augite, titanomagnetite, and glass. A xenolith of

andesitic to basaltic composition, 1 cm in diameter, was found. It contains subhedral to anhedral phenocrysts of <1.5 mm plagioclase, <0.4 mm augite, and <0.4 mm olivine, which phenocrysts are set in the groundmass composed of plagioclase, titanomagnetite, and glass.

Terayama basalt (Augite-bearing olivine basalt)

This lava flow lies on the highest position of a cliff in the south of the Yoshino-dai area, faced on the Kagoshima Bay. The flow overlies Osakibana dacite, Muregaoka andesite, and the Kekura formation, as Oki and Hayasaka (1970) reported.

Microscopically, the lava is porphyritic, in which the phenocryst phases are plagioclase, olivine, and augite. Augite is rare. Plagioclase phenocrysts are euhedral or subhedral and <3 mm in length, show twinning, and contain titanomagnetite and olivine. Olivine phenocrysts are subhedral and <1.2 mm in length. Most are altered into iddingsite. Augite phenocrysts are subhedral and <0.3 mm in length and show twinning. The groundmass is intersertal and composed of plagioclase, olivine, augite, and titanomagnetite.

Amagahana dacite (Hypersthene-hornblende dacite)

This lava dome lies at Amagahana. The dome probably overlies Muregaoka andesite.

Microscopically, the lava is porphyritic, in which the phenocryst phases are plagioclase, hornblende, hypersthene, and titanomagnetite. Plagioclase phenocrysts are subhedral and <3.5 mm in length. Most are clear or dusty, and honeycomb plagioclase is rare. The plagioclase phenocrysts show twinning and zoning and contain glass, titanomagnetite, and hornblende. Hornblende phenocrysts are euhedral or subhedral and <2 mm in length, show twinning, and contain plagioclase and titanomagnetite. Hypersthene phenocrysts are subhedral, <3.5 mm in length, and contain titanomagnetite, plagioclase, and hornblende. Titanomagnetite phenocrysts have irregular shapes and <0.8 mm in length. Some phenocrysts form crystal clusters, composed of pl + hornblende + Ti-mg + glass. The groundmass is glassy with flow structure.

3. K-Ar ages

Analytical Procedure

Samples for K-Ar dating were ground in a tungsten-carbide mortar. The sieved 60 to 80 mesh size fractions were cleaned with deionized water and then put on a hot plate at 60°C to remove Cl. They were dried in an oven at 110°C for 24 hours. From them, magnetic fractions such as iron oxides and coarse-grained plagioclase phenocrysts that often contain excess Ar were removed with a Neomax (hand-magnet) and an isodynamic separator, respectively, and then the resultant fractions were used for the Ar analysis. A portion of the fraction was ground in an agate mortar and used for K analysis. The

Table 2. K-Ar age data for the precaldera lavas in the Yoshino-dai area.

Lava name	Sample	K (wt.%)	Rad. argon 40 (10E-8ccSTP/g)	K-Ar age (Ma)	Non Rad. Ar (%)
Terayama basalt	AR-4.3	0.404±0.020	1.08±0.51	0.69±0.33	96.9
Muregaoka andesite	MY-09	2.033±0.041	6.30±0.12	0.80±0.02	41.7
Tsurugino-oka andesite	SG-92	1.513±0.030	4.73±0.30	0.81±0.05	79.0
Shirahama basalt	AR-1	0.432±0.022	1.56±0.58	0.93±0.35	95.9
Hiramatsu andesite	SH-43	1.376±0.028	2.67±0.14	0.50±0.03	74.0
Osakibana basaltic dike	AR-3.2	1.649±0.033	3.48±0.13	0.54±0.02	67.5

analyses of K and Ar, and calculations of ages and errors, were carried out at Okayama University of Science using the methods described by Nagao et al. (1984) and Itaya et al. (1991). K was analyzed by flame photometry using a 2,000 ppm Cs buffer, which has an analytical error within 2 % at the 2 σ confidence level. Ar was analyzed on a 15 cm radius sector-type mass spectrometer with a single collector system, using an isotopic dilution method and an ^{38}Ar spike (Itaya et al., 1991). The decay constants for ^{40}Ar and ^{40}Ca, and the ^{40}K content in potassium used in the age calculations are from Steiger and Jäger (1977), and are 0.581×10^{-10}/yr, 4.962×10^{-10}/yr, and 0.0001167, respectively.

Results

K-Ar ages obtained are given in Table 2. They show that the lavas in the Yoshino-dai area are a series of Aira precaldera ejecta. The age of Hiramatsu andesite is inconsistent with the stratigraphy, which cannot be explained at the present stage. The age of the Osakibana basaltic dike is interpreted to be the timing of intrusion of the dike. The ages of the basalts and andesites are >0.5 Ma. In contrast, K-Ar age of Okogashima rhyolite, precaldera rhyolite is 0.25-0.38 Ma (Tatsumi and Inoue, 1993). Precaldera pyroclastic flow deposits overlie the precaldera lavas in the Yoshino-dai area (Oki and Hayasaka, 1970), so the pyroclastic eruptions may have occurred after $\sim$ 0.5 Ma.

4. Chemical compositions

Major and trace elements (SiO_2, TiO_2, Al_2O_3, Fe_2O_3, MnO, MgO, CaO, Na_2O, K_2O, and P_2O_5; Ba, Nb, Pb, Rb, Sr, Th, Y, and Zr) were measured by RIGAKU 3070 X-ray fluorescence (XRF) spectrometer at the Graduate School of Human and Environmental Sciences, Kyoto University, following the analytical methods of Goto and Tatsumi (1991, 1992).

Representative analyses for the precaldera lavas and essential pumices in the Ito pyroclastic flow deposit as climactic ejecta are given in Table 3 and are plotted on SiO_2 variation diagrams (Fig. 4), along with Okogashima rhyolite, a precaldera rhyolite (Tatsumi and Inoue, 1993). The precaldera and climactic ejecta show approximately a single trend. For some elements, gradients of the trends change at $SiO_2 \sim 65$ wt.%. Compositions of the basalts are scattered for some elements. The Osakibana basaltic dike, which contains more olivine and less plagioclase than the other basalts, is higher in

Table 3. Representative analyses of the precaldera lavas in the Yoshino-dai area and the climactic ejecta.

Sample #	AR-1	AR-2.1	AR-3.2	AR-21	SH-43	MY-09	MY-23.1	MY-51	MY-63
Material	SB	SB	OB	TB	HA	MA	MA	MA	MA
SiO_2	50.06	51.64	49.11	50.81	59.69	60.63	59.23	60.80	58.21
TiO_2	0.91	0.84	0.91	0.96	0.77	0.71	0.71	0.68	0.73
Al_2O_3	20.60	19.53	19.39	20.41	18.30	16.38	16.49	16.39	16.56
FeO*	9.24	9.50	10.11	10.22	6.29	6.48	6.68	6.19	6.92
MnO	0.17	0.17	0.28	0.18	0.12	0.12	0.13	0.12	0.13
MgO	3.97	4.87	4.89	3.59	1.97	2.84	3.31	2.99	3.61
CaO	11.05	10.56	11.48	10.60	7.05	5.90	6.61	5.86	7.07
Na_2O	2.83	2.65	2.47	2.54	3.63	3.42	3.15	3.42	3.18
K_2O	0.44	0.41	0.40	0.55	1.43	2.00	2.08	2.02	1.80
P_2O_5	0.17	0.14	0.18	0.15	0.18	0.15	0.15	0.15	0.15
Total	99.43	100.31	99.21	100.00	99.43	98.64	98.54	98.62	98.34
FeO*	8.32	8.55	9.09	9.20	5.66	5.83	6.01	5.57	6.23
Mg#	45.93	50.35	48.94	41.04	38.22	46.46	49.56	48.85	50.77
Ba	91.4	104.5	104.4	107.2	250.8	280.7	280.8	328.3	276.9
Nb	1.8	1.7	1.6	1.5	4.7	5.9	5.7	6.3	5.1
Pb	3.8	4.2	4.5	4.6	9.9	13.2	13.4	13.4	12.1
Rb	10.5	9.8	7.3	14.9	47.2	72.5	69.2	73.4	63.6
Sr	343.9	289.4	477.9	302.7	289.0	264.2	280.3	274.5	295.2
Th	0.3	0.2	1.0	0.6	4.0	6.8	6.3	6.6	6.0
Y	21.8	19.2	19.8	20.0	25.9	33.5	29.6	29.4	27.6
Zr	71.9	63.4	68.9	57.9	145.4	162.9	154.6	165.2	144.0

Sample #	MY-64	MY-80	SG-38.3	SG-92	AR-3.3	AR-22	MY-13	MY-68	SKM
Material	MA	MA	TA	TA	OD	AD	CR	CR	CR
SiO_2	59.90	60.96	56.97	57.74	66.28	68.60	73.51	72.49	73.42
TiO_2	0.73	0.74	0.83	0.78	0.74	0.42	0.19	0.20	0.20
Al_2O_3	16.74	16.79	18.12	17.24	16.19	15.18	13.66	13.78	13.75
FeO*	6.85	6.59	7.86	7.39	5.16	3.03	1.72	1.74	1.79
MnO	0.13	0.12	0.15	0.15	0.12	0.11	0.04	0.05	0.04
MgO	3.48	2.88	2.78	3.30	1.53	0.81	0.11	0.23	0.16
CaO	6.84	6.32	7.83	7.36	4.40	3.24	1.87	2.05	2.03
Na_2O	3.18	3.29	3.44	3.23	4.22	4.10	3.80	3.91	3.68
K_2O	1.82	1.91	1.14	1.48	1.90	2.33	3.25	3.31	3.13
P_2O_5	0.15	0.16	0.17	0.16	0.20	0.12	0.06	0.06	0.06
Total	99.81	99.76	99.29	98.83	100.72	97.93	98.21	97.82	98.26
FeO*	6.16	5.93	7.07	6.65	4.64	2.72	1.55	1.57	1.61
Mg#	50.16	46.41	41.15	46.94	36.99	34.67	11.19	20.85	15.24
Ba	279.4	329.3	231.6	235.1	312.7	417.8	459.1	473.3	454.1
Nb	5.3	6.7	4.4	4.2	6.0	6.1	6.0	5.9	5.8
Pb	13.7	12.8	9.2	10.2	12.9	16.5	20.5	20.3	18.8
Rb	67.6	73.2	39.7	41.3	67.3	85.8	122.7	121.4	122.9
Sr	282.9	313.3	307.4	285.9	239.4	223.3	129.9	137.8	134.1
Th	5.4	7.1	2.4	2.7	5.9	8.1	11.8	11.8	11.5
Y	27.7	28.8	23.2	24.0	29.3	28.5	20.6	20.6	20.6
Zr	150.8	168.1	111.8	138.7	189.6	157.2	137.8	140.4	138.7

–following Table 3.–

Major elements in wt.%, trace elements in ppm.
Fe_2O_3* and FeO* correspond to total iron as Fe_2O_3 and FeO, respectively.
Mg# is equal to Mg/ (Fe + Mg).
Key to symbols for materials
SB : Shirahama basalt
OB : Osakibana basaltic dike
TB : Terayama basalt
HA : Hiramatsu andesite
MA : Muregaoka andesite
TA : Tsurugino-oka andesite
OD : Osakibana dacite
AD : Amagahana dacite
CR : Climactic ejecta (essential rhyolitic pumices in the Ito pyroclastic flow deposit)

MnO and Sr. The compositions of climactic ejecta (essential pumices in the Ito pyroclastic flow deposit) are homogeneous, as indicated formerly (Aramaki, 1984; Tsukui and Aramaki, 1990), and approximately similar to those of Okogashima rhyolite, except for K_2O and Y.

5. Discussion

As described above, a single chemical trend is observable between precaldera and climactic ejecta in the Aira caldera (Fig. 4). However, these ejecta were not produced by a single magmatic process.

A series of the precaldera and climactic magmas could be derived from basaltic magmas by fractional crystallization, which has been examined based on mass balance calculations for major elements using appropriate basalt-dacite-rhyolite sets. The calculations were carried out in two stages; (1) from basaltic to dacitic magmas through fractional crystallization of pl + cpx ± ol ± opx + mt + ilm and (2) from dacitic to rhyolitic magmas through fractional crystallization of pl + cpx + mt + ilm + ap ± qz. The division into the two stages is required by the cusp of the chemical trend. Phenocryst compositions used (Table 4) were taken from Druitt and Bacon (1989) for stage (1) and Tsukui and Aramaki (1990) for stage (2), since the phenocrysts in stage (1) rocks may have crystallized in calcalkaline andesite which has a bulk composition and mineral assemblage approximately similar to the Aira precaldera andesites and the phenocrysts in stage (2) rocks are contained in the Osumi pumice fall, one of the Aira climactic ejecta. The results of the calculations are shown in Table 5. Basaltic and andesitic mineral assemblages were used in Calc. 1-1 and 1-2, respectively, and composite assemblage, in Calc. 1-3. Dacitic and rhyolitic mineral assemblages were used in Calc. 2-1 and 2-2, respectively. The results of the calculations for stage (1) show too large Σr^2 or negative values. Thus, it is evident that the dacitic magma could not have been derived from the basaltic magma through fractionation of phenocryst phases. Moreover, fractional crystallization is inconsistent with Rb/K ratios (Fig. 5) for the precaldera ejecta. Both Rb and K are incompatible for the minerals contained in the

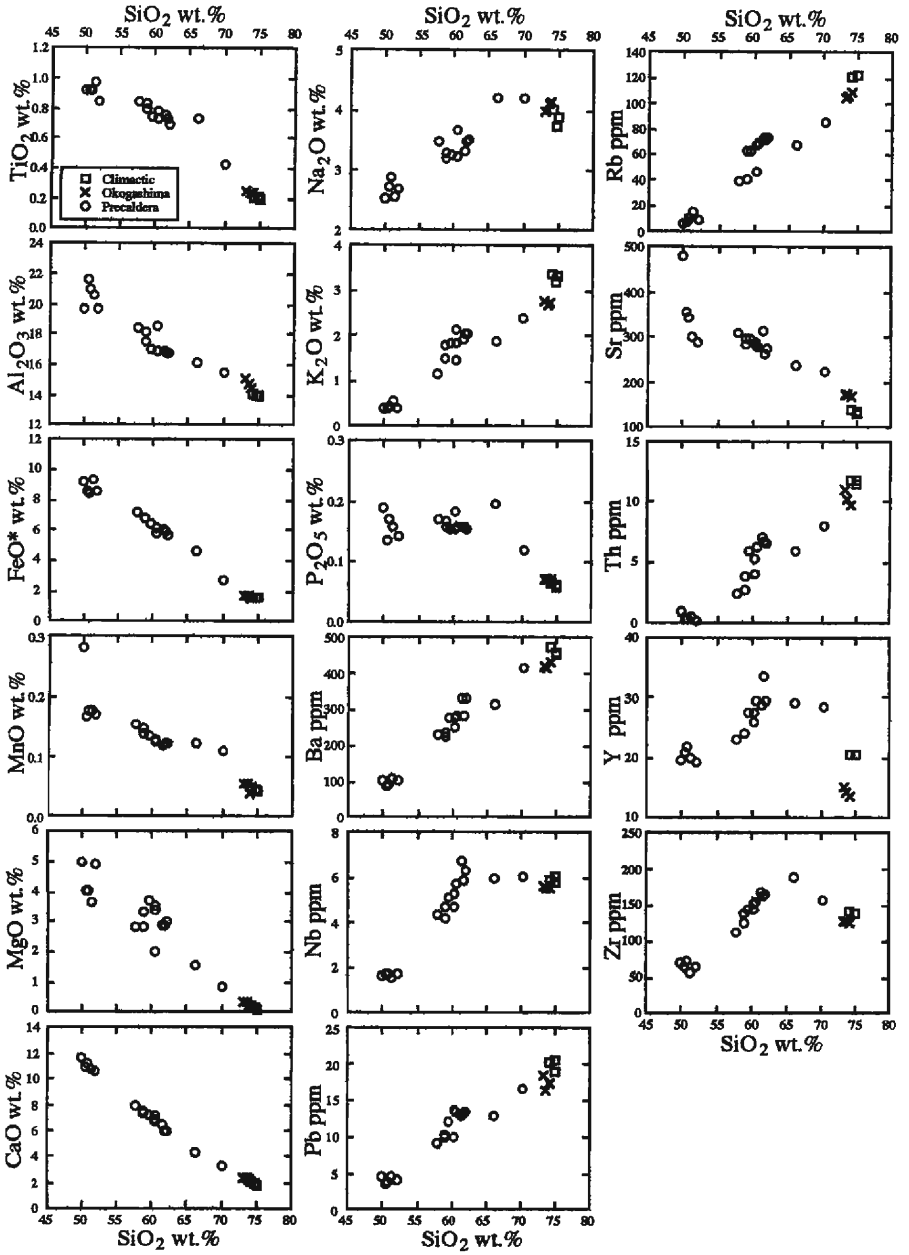

Fig. 4. SiO_2 variation diagrams. Data plotted are recalculated to total iron as FeO and then total 100 wt.% volatile free. In addition, data for Okogashima rhyolite (Tatsumi and Inoue, 1993) are plotted.

Table 4. Phenocryst compositions used for the mass balance calculations.

Pheno.	pl-1	pl-2	opx-1	opx-2	cpx-1	ol-1	mt-1	mt-2	ilm-1	ilm-2	ap	qz
SiO_2	53.80	56.79	53.50	52.62	52.10	38.40	0.07	0.21	0.03	0.00	-	100
TiO_2	-	-	0.30	0.20	0.49	-	11.20	11.64	43.50	48.06	-	-
Al_2O_3	29.00	26.31	1.34	0.64	1.70	-	2.83	1.36	0.31	0.00	-	-
FeO	0.44	0.19	17.60	26.67	7.90	17.80	78.00	81.37	49.50	49.14	-	-
MnO	-	-	0.49	0.63	0.26	0.23	0.43	0.80	0.44	1.03	-	-
MgO	0.07	-	26.00	19.03	15.80	42.70	2.65	0.17	3.95	0.95	-	-
CaO	11.50	9.11	1.27	1.13	21.10	0.09	0.02	-	0.01	-	39.66	-
Na_2O	4.93	6.36	0.02	-	0.35	-	-	-	-	-	-	-
K_2O	0.13	0.30	-	-	-	-	-	-	-	-	-	-
P_2O_5	-	-	-	-	-	-	-	-	-	-	60.34	-

Suffix. 1: in calcalkaline andesites after Druitt and Bacon (1989). 2: in Osumi pumice fall after Tsukui and Aramaki (1990).
The values for ap and qz are theoretical ones.
Abbreviations. pl:plagioclase, opx:orthopyroxene, cpx:clinopyroxene, ol:olivine, mt:magnetite, ilm:ilmenite, ap:apatite, qz:quartz.

Table 5. Results of the mass balance calculations.

Stage(1) basaltic to dacitic magmas.

Calc.1-1		Calc.1-2		Calc.1-3	
Parent: AR-1		Parent: AR-1		Parent: AR-1	
Daughter: AR-3.3		Daughter: AR-3.3		Daughter: AR-3.3	
pl-1	61.9 %	pl-1	62.1 %	pl-1	150.2 %
opx-1	2.5	ol-1	2.4	ol-1	-119.2
cpx-1	15.8	cpx-1	15.3	opx-1	228.1
mt-1	7.4	mt-1	7.4	cpx-1	8.3
ilm-1	-0.3	ilm-1	-0.3	mt-1	-6.5
AR-3.3	12.7	AR-3.3	13.0	ilm-1	5.0
$\sum r^2$	78.582	$\sum r^2$	51.772	AR-3.3	-149.3
				$\sum r^2$	10.894

Stage(2) dacitic to rhyolitic magmas.

Calc.2-1		Calc.2-2	
Parent: AR-3.3		Parent: AR-3.3	
Daughter: SKM		Daughter: SKM	
pl-2	29.0 %	pl-2	32.0 %
opx-2	7.8	opx-2	7.6
mt-2	1.2	mt-2	1.4
ilm-2	0.9	ilm-2	0.9
ap	0.5	ap	0.4
SKM	60.6	qz	2.9
$\sum r^2$	0.276	SKM	54.8
		$\sum r^2$	0.151

For the compositions of AR-1, AR-3.3, and SKM see Table 3.
$\sum r^2$ is sum of squares of residuals between observed and calculated.

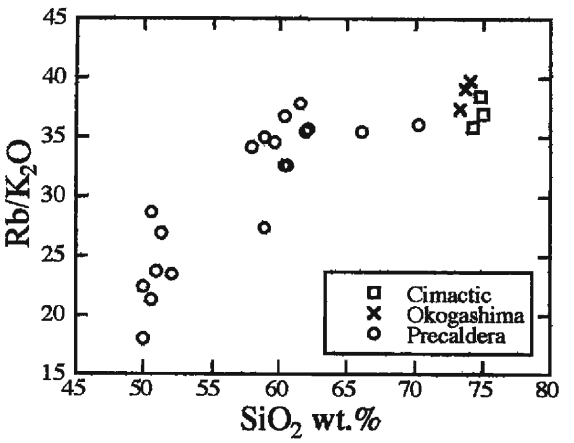

Fig. 5. SiO_2 vs. Rb/K ratio diagram. Rb and K are incompatible for plagioclase, augite, hypersthene, olivine, and titanomagnetite. Thus, if fractional crystallization of such minerals had dominated the compositions of the precaldera and climactic ejecta, the Rb/K ratio would have been constant.

Yoshino-dai lavas, suggesting a Rb/K ratio rather constant during the fractional crystallization process. But the Rb/K ratios increase with increasing SiO_2 (Fig. 5). Thus, fractional crystallization did not control the chemical compositions. In addition, the formation of $\sim$ 110 km^3 climactic rhyolitic magma by fractional crystallization requires more than 2,000 km^3 basaltic magma because the volume of rhyolitic magmas produced by fractional crystallization of basaltic magmas is only 5 wt.% of the original basaltic magma. It follows that large amounts of cumulates should exist beneath the Aira caldera to cause a significant positive gravity anomaly. However, negative gravity anomaly was reported there (Yokoyama and Ohkawa, 1986). Also, magma mixing of two end members, the most basaltic and the most felsic magmas, is unlikely, because such a process may not form a geochemical cusp in the variation diagrams at $\sim$ 65 SiO_2 wt.% (Fig. 4).

Multiple processes must have been involved for the production of a series of precaldera and climactic ejecta in Aira caldera. The K-Ar ages of the precaldera ejecta show that basaltic to andesitic volcanism ceased at $\sim$ 0.5 Ma and that only felsic volcanism has existed since $\sim$ 0.5 Ma. It is possible that the state of the magmatic system beneath the Aira caldera may have changed at $\sim$ 0.5 Ma; for example, supply of basaltic magma from the mantle ceased, or the formation of a felsic magma chamber prevented more mafic magmas from erupting. It follows that different processes controlled the production of basaltic to andesitic magmas before $\sim$ 0.5 Ma, and of dacitic to rhyolitic magmas after $\sim$ 0.5 Ma. Magma mixing for production of the precaldera intermediate magmas or partial melting of crustal material for production of felsic magmas may be considered such processes.

6. Conclusions

(1) Precaldera lavas in the Yoshino-dai area mainly consist of augite-olivine basalt and two-pyroxene andesite, as previous workers indicated. Dacite lavas are distributed in Osakibana and Amagahana. Hiramatsu basalt and Osakibana andesite must be renamed 'Hiramatsu andesite' and 'Osakibana dacite', respectively because of their chemical compositions ($SiO_2 \sim 60$ wt.% for Hiramatsu andesite and $SiO_2 \sim 66$ wt.% for Osakibana dacite).

(2) A series of Aira precaldera magmas was not produced by a single differentiation process such as fractional crystallization from basaltic magmas or two-end-member mixing between basaltic magmas and rhyolitic magmas. Generation of a series of Aira precaldera magmas requires at least two processes; production of basaltic to andesitic magmas before ~ 0.5 Ma and of dacitic to rhyolitic magmas after ~ 0.5 Ma. In other words, it is possible to consider that the state of the magmatic system beneath the Aira caldera may have changed at ~ 0.5 Ma

Acknowledgements

—We are grateful to the staff at Sakurajima Volcanological Observatory, Kyoto University for letting us use the facilities at the observatory. We thank Miss R. Arai for reviewing the English of this manuscript.

References

Aramaki, S. (1984): Formation of the Aira Caldera, Southern Kyushu, ~ 22,000 Years Ago, J. Geophys. Res., Vol. 89, pp. 8485-8501.

Druitt, T. H. and C. R. Bacon (1989): Petrology of the zoned calcalkaline magma chamber of Mount Mazama, Crater Lake, Oregon, Contrib. Mineral. Petrol., Vol. 101, pp. 245-259.

Goto, A. and Y. Tatsumi (1991): Quantitative analysis of rock samples with a X-ray fluorescence apparatus (I), The Rigaku-Denki Journal, Vol. 22, pp. 28-44 (in Japanese).

Goto, A. and Y. Tatsumi (1992): Quantitative analysis of rock samples with a X-ray fluorescence apparatus (II), The Rigaku-Denki Journal, Vol. 23, pp. 50-69 (in Japanese).

Hildreth, W. (1981): Gradients in Silicic Magma Chambers: Implications for Lithospheric Magmatism, J. Geophys. Res., Vol. 86, pp. 10153-10192.

Inoue, H. (1992): Geology and Petrology of Volcanic Rocks in the Northern Part of Yoshino-dai, the Northwestern edge of the Aira Caldera, Graduate Thesis, Kyoto Univ. (in Japanese).

Itaya, T., K. Nagao, K. Inoue, Y. Honjou, T. Okada, and A. Ogata (1991): Argon isotope analysis by a newly developed mass spectrometric system for K-Ar dating, Mineral. J., Vol. 15, No. 5, pp. 203-221.

Kobayashi, T., A. Iwamatsu, and T. Tsuyuki. (1977): Volcanic Geology of the Aira Caldera Wall and Slope Disasters Which Recently Occurred on It, Rep. Fac. Sci., Kagoshima Univ. (Earth Sci. Biol.), Vol. 10, pp. 53-73 (in Japanese).

Matumoto, T. (1943): The Four Gigantic Caldera Volcanoes of Kyusyu, Japanese Journal of Geology and Geography, Vol. 19, Special No., pp. 1-57.

Nagamune, T. (1987): Intermediate-Depth Earthquakes and Tectonics of the Kyushu-Ryukyu Region, J. Seismol. Soc. Jpn., Vol. 40, pp. 417-423 (in Japanese).

Nagao, K., H. Nishido, T. Itaya, and K. Ogata (1984): An Age Determination by K-Ar Method, Bull. Hiruzen Res. Inst., Vol. 9, pp. 19-38 (in Japanese).

Oki, K. and S. Hayasaka (1970): Quaternary Stratigraphy in the Northern Part of Kagoshima City, Rep. Fac. Sci., Kagoshima Univ. (Earth Sci. Biol.), Vol. 3, pp. 67-92 (in Japanese).

Steiger, R. H. and E. Jäger (1977): Subcommission on Geochronology: Convention on the Use of Decay Constants in Geo- and Cosmochronology, Earth Planet. Sci. Lett., Vol. 36, pp. 359-362.

Tatsumi, Y. and H. Inoue (1993): Rhyolite from Okogashima Island, Kagoshima Prefecture－K-Ar ages and Petrological Characteristics－, Annuals Disas. Prev. Res. Inst., Kyoto Univ., No. 36, pp. 231-236 (in Japanese).

Tsukui, M. and S. Aramaki (1990): The Magma Reservoir of the Aira Pyroclastic Eruption－A Remarkably Homogeneous High-Silica Rhyolite Magma Reservoir, Bull. Volcanol. Soc. Jpn., Vol. 35, pp. 231-248 (in Japanese).

Yamaguchi, K. (1975): Study of Sakurajima volcanoes－Geological and petrological studies of regions around Kagoshima Bay and Sakurajima volcanoes, Nihon Chigaku Kyoiku Gakkai, Tokyo, p. 128 (in japanese).

Yokoyama, I. and S. Ohkawa (1986): The subsurface structure of the Aira caldera and its vicinity in southern Kyushu, Japan, J. Volcanol. Geotherm. Res., Vol. 30, pp. 253-282.